Molecular vibrational analysis and MAS-NMR spectroscopy study of epilepsy drugs encapsulated in TiO2-sol-gel reservoirs

ARTICLE *in* JOURNAL OF BIOMEDICAL MATERIALS RESEARCH PART A · SEPTEMBER 2006

Impact Factor: 3.37 · DOI: 10.1002/jbm.a.30842 · Source: PubMed

Molecular vibrational analysis and MAS-NMR spectroscopy study of epilepsy drugs encapsulated in TiO_2-sol–gel reservoirs

T. Lopez,[1,2] J. Navarrete,[3] R. Conde,[3] J.A. Ascencio,[3] J. Manjarrez,[2] R.D. Gonzalez[4]
[1]*Universidad Autonoma Metropolitana—Iztapalapa, P.O.Box 55–534, Mexico, D.F. 09340, Mexico*
[2]*Instituto Nacional de Neurologia y Neurocirugia "Manuel Velazco Suarez", Av. Insurgentes Sur 3877 C.P., Mexico, D.F. 14269, Mexico*
[3]*Instituto Mexicano del Petroleo, Eje Central Lazaro Cardenas 152, San Bartolo Atepehuacan, Mexico, D.F. 07730, Mexico*
[4]*Department of Chemical Engineering, Tulane University, New Orleans, Louisiana 70118*

Received 21 March 2005; revised 29 August 2005; accepted 12 October 2005
Published online 23 May 2006 in Wiley InterScience (www.interscience.wiley.com). DOI: 10.1002/jbm.a.30842

Abstract: A nanostructured matrix, consisting of titania, was designed in such a way that an antiepileptic drug could be encapsulated and released according to a well-defined time release schedule. The titania was synthesized by a sol–gel method in which titanium *n*-butoxide was used as the precursor for the formation of the sol. The synthesis was optimized to yield a homogeneous particle size with a high porosity and an anatase crystal structure. The antiepilectic drugs, phenytoine or valproic acid, were added during the gelation stage in order to obtain a homogeneous gel phase. The resulting nanostructured matrix including the drug showed only weak attractive forces, such as London forces, dipole–dipole coupling, and in some cases hydrogen bonds. The resulting assembly, referred to as a reservoir, was characterized using conventional FTIR and NMR spectroscopic techniques. Theoretical simulation studies were performed so as to obtain an understanding of the equilibrium electrostatic potential distribution and the relative charges on the titania and the anticonvulsants. © 2006 Wiley Periodicals, Inc. J Biomed Mater Res 78A: 441–448, 2006

Key words: sol–gel; TiO_2; epilepsy; drug delivering; molecular vibrational analysis; nanostructured reservoir; quantum mechanics calculations

INTRODUCTION

Temporal lobe epilepsies (TLE) are the most frequent in pharmacoresistant epilepsy (ILAE, International League Against Epilepsy Commission, 1989). For this reason, research into TLE and the evaluation of the classification system of TLE are of special interest, because they contribute to a deeper understanding of treatment schedules in TLE. The development of diagnostic techniques, such as magic angle spinning–nuclear magnetic resonance (MAS-NMR) spectroscopy, may offer the possibility of improving the evaluation of current classification systems. Several classification schemes consisting of subgroups in TLE exist.[1–3] The international classification of epilepsy syndromes (1989) distinguishes between mesiobasal TLE and lateral (neocortical) TLE. A question arises as to whether new image techniques are able to distinguish between mesial and lateral TLE in lesion patients. Recent studies provide strong evidence that metabolic differences between mesial and lateral TLE in hippocampal regions exist and it is difficult to establish differences between them. For this reason, it is still necessary to continue implementing study techniques for the TLE.[4–7] At the same time, it is necessary to continue treating patients with appropriate anticonvulsive drugs, using the best administration procedure, to achieve maximum effectiveness.

Monotherapy remains the preferred method in epilepsy treatment, albeit some effective strategies of adjunctive or combined treatment of patients with intractable seizures have been developed.[8] However, there is still no accepted consensus on how to treat patients with refractory or unsatisfactorily medicated seizures effectively. Based on experimental studies on animals and pharmacological presumptions regarding mechanisms of the action of available antiepileptic drugs, the rationale for polytherapy, in epilepsy treat-

Correspondence to: T. López; e-mail: tesy@xanum.uam.mx, tlopez@innn.edu.mx; or J.A. Ascencio; e-mail: ascencio@imp.mx

ment, allows one to predict the drug combinations that might be effective on patients resistant to standard medication.[9]

In the last 10 years, a novel and very effective way of administering drugs has been investigated by several researchers.[10–12] This process consists in the synthesis of a suitable material in which the physical, chemical, textural, and structural properties can be controlled. The proper control of these properties can be used to vary the rate of drug release. One such system was found to consist of polyanhydrides, in particular, poly(fumaric-cosebacic anhydride). Previous research has focused on the bioadhesive interactions of the copolymer with mucosal tissue.[13] Following these observations, many studies have been performed using different copolymers. Several of these have turned out to be quite effective.[14]

With the aid of theoretical simulations, it is possible to calculate and interpret electronic and atomistic structures and show how they can affect the corresponding chemical interactions between materials.[15,16] These interactions determine the chemical selectivities and the possible reactions between species.[17] In particular, density functional theory (DFT) has been found to be useful in the analysis of molecules and the possible interactions between organic–inorganic materials.[18]

In the present study, the use of an inorganic reservoir consisting of TiO_2 prepared by a sol–gel technique as a replacement for the polymeric materials will be tried. Ti and Ti alloys are corrosion-resistant and light, yet sufficiently strong for use as load bearing and machinable orthopedic implant material. They are one of the biocompatible metals that oseointegrate (direct chemical or physical bonding with adjacent bone surfaces without forming a fibrous tissue interface layer). For this reason, it has been successfully used as orthopedic and dental implants. Typical antiepileptic drugs, such as phenytoine (Ph) and valproic acid (VH), will be encapsulated within the titania matrix, and the drug–titania interactions will be characterized using standard spectroscopic techniques. In order for the implants to be useful, the host-matrix implants must be biocompatible. The accepted definition of biocompatibility is "the ability of a material to perform with appropriate host response in a specific application." For this reason, it is absolutely essential that the host drug must be biocompatible with the titania matrix. In order for biocompatibility to be achieved, it is important that the structure of the host drug remains intact as a result of the interaction with the titania matrix. During the course of this study, the structure of the host will be probed by physical methods to ensure biocompatibility.

Owing to recent advances in the area of medical technology, it has become desirable to synthesize new materials with different physical and chemical properties to meet these new requirements. The sol–gel method represents an excellent approach to obtain nanomaterials used as drug reservoirs for drug release control. The process takes place in two steps: the first of which is the hydrolysis of an alkoxide precursor.

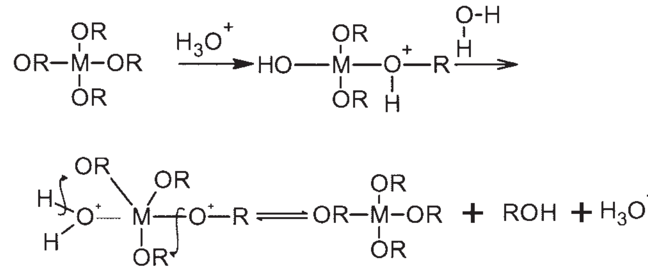

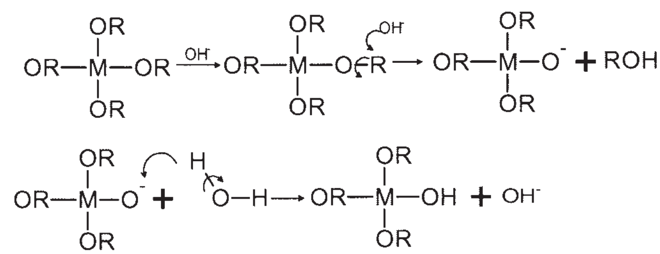

The second step is a polymerization reaction. In this step, it is possible to control the properties of the resulting gel. This includes the required texture, structure, and the required polarity of the material so as to obtain a final product having the correct drug release properties.

release properties.

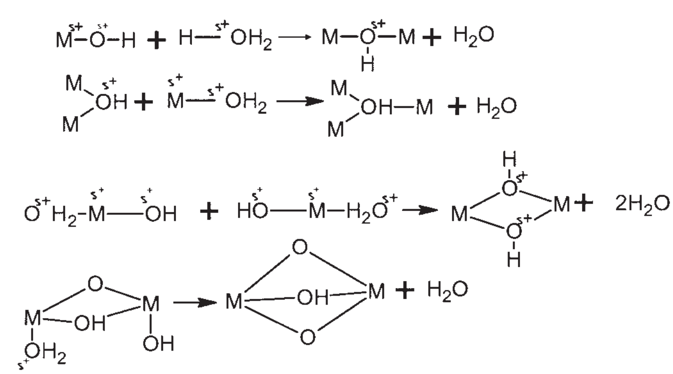

EXPERIMENTAL AND THEORETICAL METHODS

Sol–gel titania synthesis

The titania reservoirs were synthesized according to the following procedure: to a reflux glass system containing 200 mL of *tert*-butyl alcohol (Baker 99.9%) and 200 mL of doubly distilled water, ammonium hydroxide was added in a dropwise manner until a pH of 9 was reached. In a separate

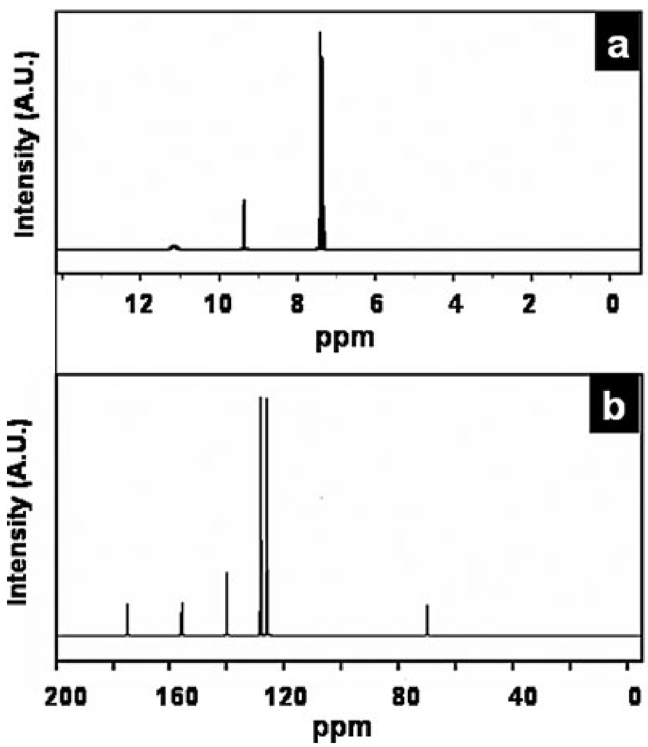

Figure 1. NMR spectra of Ph obtained in solution: (a) ^{1}H and (b) ^{13}C.

reflux reactor, thermostated at 35°C and under conditions of constant stirring, 84.5 mL of titanium tetra-*n*-butoxide (Aldrich 98%) were added in a dropwise fashion over a 24-h period, while the temperature was maintained at 35°C. The resultant gel was dried under vacuum conditions at 40°C in a rotavapor (and henceforth denoted as a fresh sample).

TiO_2-Ph and TiO_2-VH synthesis

The synthesis of the encapsulated drug–titania reservoirs was performed as follows: to a reflux glass system which contained 200 mL of *tert*-butyl alcohol (Baker 99.9%), 200 mL of doubly distilled water, containing either dissolved sodic Ph or VH, was added. The pre-gel containing the sodic Ph had a pH of 9 while that containing the VH had a pH of 2. Separately, in a reflux thermostatic reactor at 35°C, 84.5 mL of titanium tetra-*n*-butoxide (Aldrich 98%) was added in a dropwise manner over a period of 24 h, under continual stirring at 35°C. The resultant gel was dried under vacuum at 35°C by means of a rotavapor.

FTIR spectroscopy

Infrared spectra of TiO_2-VH and TiO_2-Ph were obtained using self-supporting wafers ($\sim$11 mg/cm^2). The wafers were positioned in a Pyrex cell equipped with cesium iodide windows. The samples were evacuated to a pressure of 1×10^{-6} torr and heated overnight at 40°C to remove water. The same sample was subsequently heated under the same conditions at 50 and 60°C. FTIR spectra were obtained using a Nicolet, Model 710, spectrophotometer in which 150 scans were coadded. The resolution was 4 cm^{-1} or better. A pure VH spectrum was obtained using a film, while Ph was obtained using KBr as a diluent.

NMR-MAS spectral analysis

MAS-NMR analysis was performed using pulse experiments in an AVANCE 400 (9.39 T) apparatus manufactured by Brucker. It was equipped with a 4-mm probe. The TiO_2-VH and TiO_2-Ph were packed in a zirconia sampler and spun at 10 kHz. Pure drugs were analyzed in the liquid phase using DMSO, with Ph and VH in $CDCl_3$. In both cases, TMS was used as a standard.

Theoretical methods: Tasks and approaches used

Structural models were obtained based on the anatase unit cell. Models of inorganic matrixes were considered for both phases in order to generate cluster configurations. Searching for an energy minimum geometrically optimized these configurations. The electronic structure was then calculated to determine the Fukui fields (electrophilic, nucleophilic, and radical sites). The calculations were made by using the Dmo13 software as part of Cerius 2 by Accelrys,[19] which is based on DFT with the local density approximation and the Perdew–Wang functional. A double-numeric quality basis set with polarization functions and basis sets (DND basis) was used with a self-consistent field convergence of 1×10^{-4} au. The models of cluster systems were compared to those made for the crystalline cell in order to evaluate the electronic and chemical differences between them and how the OH production improves the biocompatibility of the sol–gel synthesized material. The corresponding calculations were made for Ph and VH, taking into account the changes in the electronic structure when it interacts with an inorganic material such as that used for the reservoir.

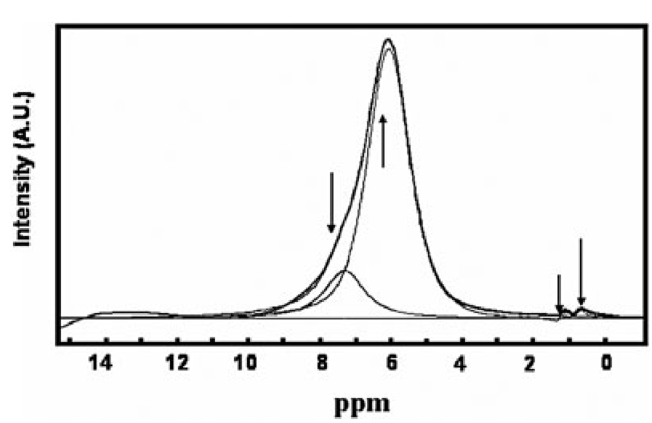

Figure 2. MAS-^{1}H-NMR spectrum of Ph/TiO_2.

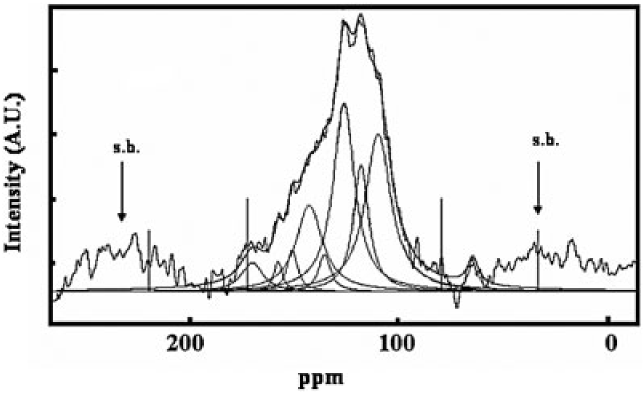

Figure 3. ^{13}C MAS-NMR spectrum of Ph/TiO_2. Side bands (s.b.) are generated by the spinning of the sample.

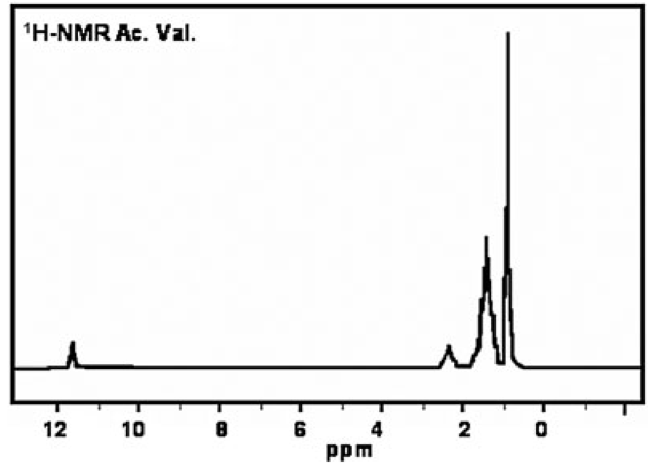

Figure 4. ^{1}H-NMR spectrum of VH in solution.

RESULTS AND DISCUSSION

NMR and MAS-NMR studies

The resultant reservoirs were studied using techniques that enable the NMR measurement of solids. One such technique is MAS. This technique enables one to obtain information from solids. This is particularly useful for samples that do not exhibit long-range order or those that consist of fine powders. In this case, chemical shift resolved spectra were obtained through the rapid rotation of the sample around an angle, which is inclined at the magic angle ($\theta = 54.7$), with respect to the applied magnetic field (B_o). This chemical shift resolved spectrum is due to the angular dependence of many spin interactions.

The ^{1}H and ^{13}C NMR spectra of Ph in solution are shown in Figure 1. In the case of the ^{1}H NMR, the most intense signal at 7.4 ppm is due to the aromatic protons. Protons linked to nitrogen give a signal at 9.4 and 11 ppm [Fig. 1(a)]. The ^{13}C NMR shows several signals in the 120–140 ppm range. The signals centered at ~130 ppm are due to aromatic carbon atoms, while the signal centered at 140 ppm is due to the C atom attached to the phenyl group. Carbonyl groups give signals at 156 and 175 ppm, and the quaternary carbons give the smallest signal that is centered at 70 ppm [Fig. 1(b)].

The ^{1}H MAS-NMR spectrum of TiO_2-Ph is shown in Figure 2. Deconvolution of the intense broad band results in two bands centered at 6 ppm, with a small shoulder at 7.75 ppm. These peaks are assigned to protons, which are bonded to the aromatic ring of Ph. A slight shift in the signals with respect to the spectrum of the same drug in solution is observed. However, both peaks assigned to protons bonded to nitrogen atoms show a large shift and appear as a doublet centered at 1 ppm.

The ^{13}C MAS-NMR spectrum of the TiO_2-Ph system is shown in Figure 3. A broad band between 180 and 100 ppm dominates the spectrum. There is a distinct doublet centered at 120 and 125 ppm, which is due to the aromatic carbon atoms. Deconvolution of this band, to several overlapping bands, is due to nuclear spin interactions. In addition to these bands, a small signal centered at 64 ppm is also observed. The band centered at ~40 ppm is due to the quaternary carbon of the molecule. It is shifted to a lower ppm than that corresponding to the same carbon atom in solution (70 ppm). In general, the spectral profile is quite similar to that obtained in solution. However, it is slightly shifted to lower ppm. This suggests that there are no significant changes between the structure of Ph in solution and that observed on TiO_2. The only significant change that occurs is in the behavior of the protons, which are linked to both nitrogen atoms. This may be due to the interaction between the host titania and the Ph. It is important to note that the use of the sol–gel process leads to a rather large concentration of surface hydroxyl groups.[20–22] This may lead to the formation of acid–base linkages such as N[b]···H—O—Ti.

The ^{1}H NMR spectrum of VH in solution is shown in Figure 4. Proton resonance peaks assigned to CH_3, CH_2, and CH occur at 1, 1.5, and 2.5 ppm respectively,

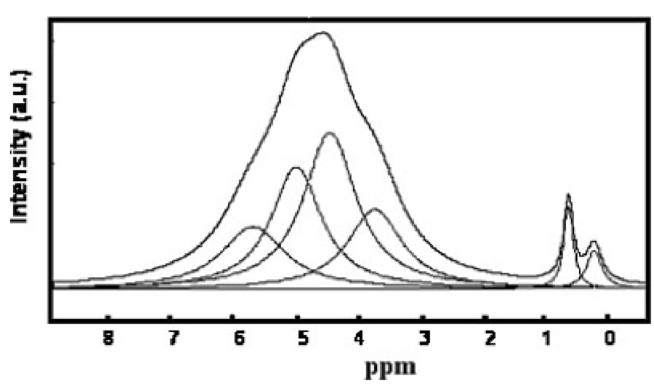

Figure 5. ^{1}H-MAS-NMR spectrum of VH/TiO_2.

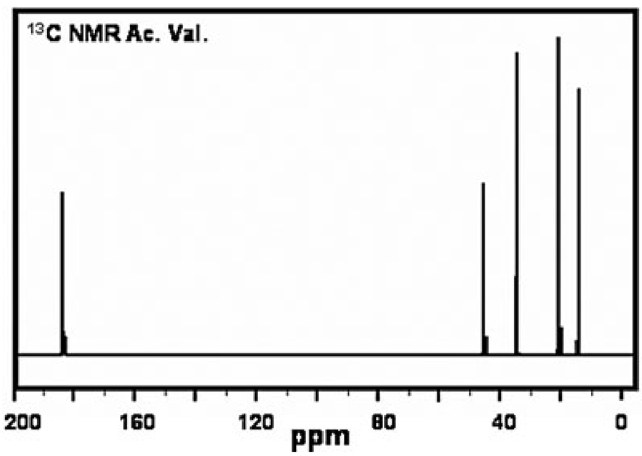

Figure 6. ^{13}C NMR spectrum of VH in solution.

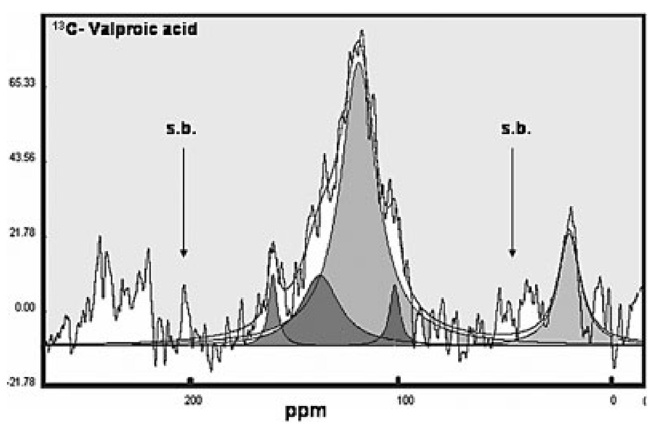

Figure 7. ^{13}C-MAS-NMR spectrum of VH/TiO_2.

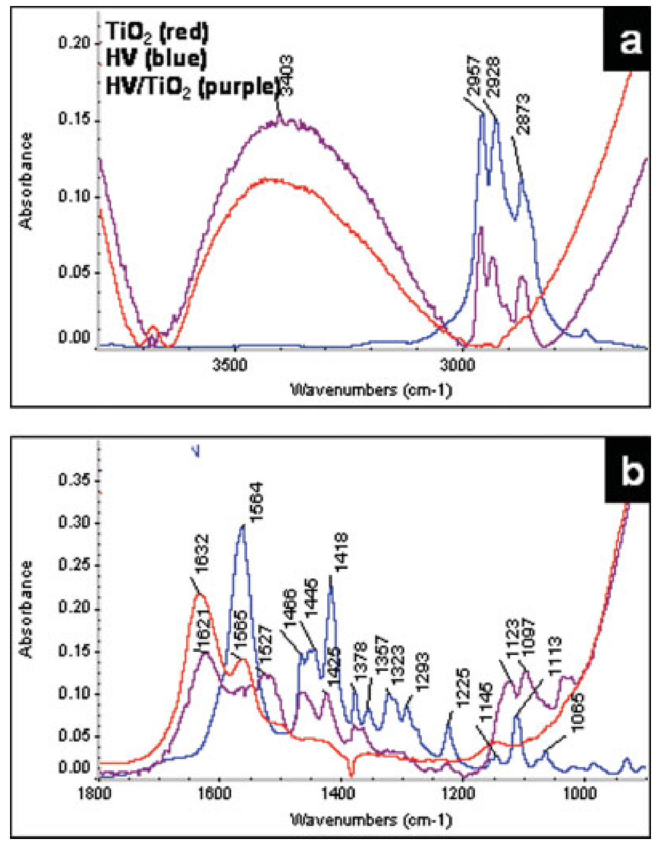

Figure 9. The infrared spectrum of TiO_2 (red line), VH (blue line), and VH/TiO_2 (purple line). (a) 4000–2500 cm^{-1} region and (b) 1800–1200 cm^{-1}region. [Color figure can be viewed in the online issue, which is available at www.interscience.wiley.com.]

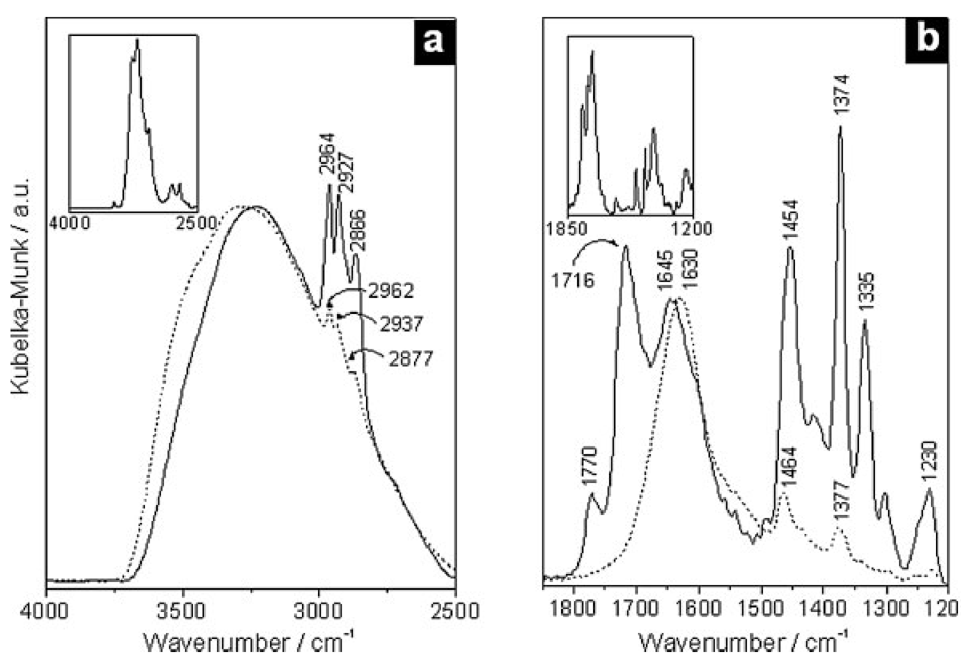

Figure 8. The infrared spectrum of Ph (solid line) and Ph/TiO_2 (dotted line). (a) 4000–2500 cm^{-1} region and (b) 1800–1200 cm^{-1}region.

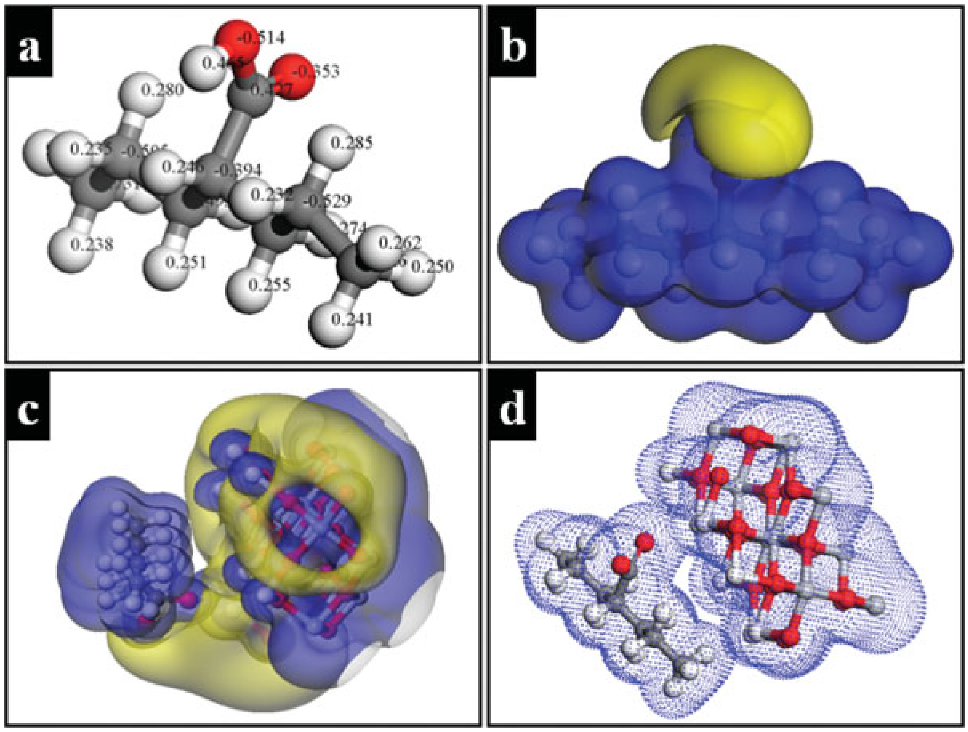

Figure 10. (a) Charge distribution and (b) electrostatic potential of the lowest energy state of VH. (c) Charge distribution and (d) electrostatic potential of the lowest energy state of Ph. (e) electrostatic potential and (f) charge density distribution of a drug molecule in response to TiO_2 surface. Yellow regions correspond to a negative polarization, while blue corresponds to a positive polarization.

while the proton resonance corresponding to the carboxylic acid group is observed at 11.5 ppm.

The ^1H MAS-NMR results for the VH/TiO_2 system is shown in Figure 5. The proton resonances corresponding to the CH_3 and CH_2 groups are slightly shifted to lower ppm and the signal corresponding to the OH group has disappeared. In addition, there is a large broad resonance peak between 3 and 7 ppm. This broad peak is due to the water pertaining to the titania. The reason for the disappearance of the proton signal associated with the OH group is that it is continually exchanging with water and the hydroxyl groups corresponding to the titania.

The ^{13}C NMR of the VH in solution is shown in Figure 6. The carbon atom of the carbonyl group, in solution, shows a significant peak at 183.5 ppm. The tertiary carbon atom of the aliphatic chain is centered at 45.5 ppm. Chemically different methylene groups show peaks at 34 and 20 ppm while the peak assigned to the methyl groups is centered at 14 ppm.

The ^{13}C MAS-NMR spectrum of VH/TiO_2 is shown in Figure 7. In addition to the large broad band centered at 120 ppm, signals centered at 159 and 17.5 ppm are also observed. The large peak centered at 120 ppm can be assigned to the carbon atoms corresponding to the carbonyl group. The methyl groups in all likelihood generate the band centered at 17.5 ppm. The small side band centered at 159 ppm is most likely associated with a carbonyl group in a somewhat different environment. The rather large shift associated with the carbonyl carbon atom is somewhat surprising. However, this rather large shift may be due to the interaction between the carbonyl atom in VH and the hydroxyl groups associated with the titania. Further evidence for this will be discussed in connection with the infrared study.

Infrared studies

The FTIR spectrum of Ph/TiO_2 in the absorbance mode is shown in Figure 8. The presence of the organic phase within the TiO_2 matrix is clearly evident as shown in the 4000–2500 cm^{-1} region of the spectrum [Fig. 7(a)]. The 1800–1200 cm^{-1} region of the spectrum is shown in Figure 7(b). The salient feature in this region is the disappearance of the carbonyl band centered at 1716 cm^{-1}. The solid line in Figure 7 represents the infrared spectrum of pure Ph while the dotted line represents the spectrum of Ph adsorbed on the host titania matrix. It is important to note that that the lower wavenumber bands associated with Ph are exactly reproduced when it is adsorbed on titania, although they are considerably weaker due to the rather low concentration of the drug on the titania.

The sharp infrared bands located between 1650 and 1300 cm^{-1} are due to the bending vibrations of CH and NH groups in Ph. The disappearance of the carbonyl band centered at 1716 cm^{-1} strongly suggests that there is a strong interaction between the adsorbed Ph molecule and the titania host, and that this interaction involves the carbonyl group of Ph with the hydroxyl groups of titania.

The infrared spectra of VH on titania is shown in Figure 9. The infrared spectrum in the 4000–2500 cm^{-1} is shown in Figure 9(a) while the spectrum in the 1800–1200 cm^{-1}. As in the case of the Ph/TiO_2 system, the solid line represents the spectrum of pure VH while the dotted line represents the spectrum of VH/TiO_2. The similarity between the Ph/TiO_2 and the VH/TiO_2 is striking. For the case of the VH, the carbonyl band, observed at a lower wavenumber because of the resonant structure of the carbonyl group (1564 $cm^{-1)}$ is completely missing from the spectrum of the VH/TiO_2 spectrum. We can therefore conclude that the interaction between VH and titania also occurs between the carbonyl group on the acid and the hydroxyl groups of the titania. The spectra of VH and VH/TiO_2 in the 1500–1200 cm^{-1}region are virtually unchanged. However, there is a decrease in intensity of the bands due to the rather low concentration of VH in the adsorbed state.

Theoretical insights

In order to obtain additional insight on drug–acceptor interactions, a DFT study was performed on both sodic Ph/TiO_2 and VH/TiO_2. Figure 10 shows the lowest configuration of VH in addition to the corresponding electrostatic potential isosurface [Fig. 10(a,b) respectively]. Similarly, the structure of Ph is shown in Figure 10(c,d). Calculations based on the drug–titania interactions are shown in the Figure 10(e, f). Owing to the configuration of the drug, the effect of polarization for the VH molecule is made based on the orientation of the oxygen atoms [red in Fig. 10(a)], which carry the largest negative charge (yellow surface). This can be verified by observing the electrostatic potential distribution [Fig. 10(b)].

A similar effect is observed for the case of Ph, where the polarization is induced by the N and Na atoms (blue and purple, respectively) in Figure 10(c,d). The positive regions have the greatest exposure [Fig. 10(d)]. The carbon rings, on the other hand, are uniformly charged.

In the presence of an inorganic surface such as titania, the interaction can be distinguished by the electrostatic potential [Fig. 10(e)], which is equilibrated in both negative and positive potentials (blue surface). The charge distribution [Fig. 10(f)] shows that only weak bonding can occur. This is completely in accord with the infrared results which show that interaction between the host and matrix occur through weak interactions between carbonyl groups and the titania surface. Perhaps these interactions are nothing more than hydrogen bonds.

CONCLUSIONS

Several important conclusions emerge from this study as follows:

1. The synthesis of the encapsulated drugs can be performed under temperature and pH conditions, which ensure that that the drug does not undergo substantial modifications.
2. Because of weak interactions between the drug and the inorganic matrix, this configuration is well suited for controlled time release.
3. For this reason, this configuration makes this an excellent candidate for use as a controlled implant for the control of epilepsy.

References

1. Walczak T. Neocortical temporal lobe epilepsy: Characterizing the syndrome. Epilepsia 1995;36:633–635.
2. O'Connor MJ, Sperling M, Liporace J, Sirven J, Freese A. Mutiple subpial transection: An adjunct to resective surgery for epilepsy in eloquent cortex. Epilepsia 1999;40:76–76.
3. Williamson P, Engel J, Munari C. Anatomic classification of localization-related epilepsies. In: Engel J, editor. Epilepsy: A Comprehensive Textbook, Vol. 3. New York: Lippincott-Raven Press; 1998. pp 2405–2416.
4. Ebersole JS, Wade PD. Spike voltage topography identifies two types of frontotemporal epileptic foci. Neurology 1991;41:1425–1433.
5. Henry T, Sutherling W, Engel J. Interictal cerebral metabolism in partial epilepsies of neocortical origin. Epilepsy Res 1991;10: 174–182.
6. Stefan H, Feichtinger M, Pauli E. Magnetic resonance spectroscopy and histopathological findings in temporal lobe epilepsy. Epilepsia 2001;42:41–46.
7. Hitten P, Druchrow R, Lanerolle NC, Spencer S. Epilepsy treatment. Epilepsia 2001;42:725–730.
8. Perucca E. Pharmacological principles as a basis for polytherapy. Acta Neurol Scand 1995;162:31–34.
9. Schmidt D. Rational polytherapy. Baillieres Clin Neurol 1996; 5:757–763.
10. Engel JJ, Van Ness P, Rasmussen T, Ojemann L. Outcome with respect to epileptic seizures. In: Engel J Jr, editor. Surgical Treatment of the Epilepsies, 2nd ed. New York: Raven Press; 1993. pp 609–621.
11. Benbadis SR, So NK, Antar MA, Barnett GH, Morris HH. The value of PET scan (and MRI and Wada test) in patients with bitemporal epileptiform abnormalities. Arch Neurol 1995;52: 1062–1068.
12. Bohnen NI, O'Brien TJ, Mullan BP, So EL. Cerebellar changes in partial seizures: Clinical correlations of quantitative SPECT and MRI analysis. Epilepsia 1998;39:640–650.

13. Cendes F, Caramanos Z, Andermann F, Dubeau F, Arnold DL. Proton magnetic resonance spectroscopic imaging and magnetic resonance imaging volumetry in the lateralization of temporal lobe epilepsy: A series of 100 patients. Ann Neurol 1997;42:737–746.
14. Koepp MJ, Richardson MP, Labbe C, Brooks DJ, Cunningham VJ, Ashburner J, Van PW, Revesz T, Duncan JS. 11C-flumazenil PET, volumetric MRI, and quantitative pathology in mesial temporal lobe epilepsy. Neurology 1997;49:764–773.
15. Ferro-Flores G, Ramírez FD, Tendilla JI, Pimentel-González G, Murphy CA, Meléndez-Alafort L, Ascencio JA, Croft BY. Preparation and pharmacokinetics of samarium (III)-153-labeled DTPA-bis-biotin. Characterization and theoretical studies of the samarium(III)-152 conjugate. Bioconjug Chem 1999;10:726–734.
16. Ascencio-Gutiérrez JA, Pérez-Marín L, Otazo Sánchez E, Castro M, Contreras-Pulido D, Cisneros GA. Molecular and quantum mechanics calculations for the 1-furoyl-3-phenylthiourea as a Pb^{2+} sensor. Afinidad 2000;487:180–184.
17. Lapinski L, Nowak MJ, Kwiatkowski JS, Leszczynski J. Phototautomeric reaction, tautomerism, and infrared spectra of 6-thiopurine. Experimental matrix isolation and quantum-mechanical (conventional ab initio and density-functional theory) studies. J Phys Chem A 1999;103:280–288.
18. Ascencio JA, Rodriguez-Lugo V, Angeles C, Santamara T, Castano VM. Theoretical analysis of hydroxylapatite and its main precursors by quantum mechanics and HREM image simulation. Comp Mat Sci 2002;25:413–426.
19. Accelrys. DMol3 module of Cerius^2. San Diego: Accelrys; 1999.
20. Lopez T, Gomez R, Sanchez E, Tzompantzi F, Vera L. Photocatalytic activity in the 2,4-dinitroaniline decomposition over TiO_2 sol–gel derived catalysts. J Sol-Gel Sci Technol 2001;22: 99–107.
21. Podbielska H, Ulatowska-Jarza A, Holowacz I. Sol–gel applicators for medical light therapy. Phys Med 2004;20:37–39.
22. Navarrete J, López T, Gómez R, Figueras F. Surface acidity of sulfated TiO_2-SiO_2 sol–gels. Langmuir 1996;12:4385–4390.